Research Article

Thermodynamics Associated with Monitoring Pre-nucleation Aggregation at High Supersaturation

Amber Laird[1], Alan Laird[1], Mahavir Chougule[1]*, Mazen Hamad[2], Kenneth R Morris[1]
[1]Department of Pharmaceutical Sciences, College of Pharmacy, University of Hawaii at Hilo, 34 Rainbow Drive, Hilo, HI 96720, USA.
[2]Department of Chemistry, University of Hawai'i at Hilo, 200 W. Kawili ST, Hilo, HI 96720, USA.
***Corresponding author's E-mail:** mahavirchougule@gmail.com

Accepted on: 01-11-2012; **Finalized on:** 31-12-2012.

ABSTRACT

The purpose is to determine thermodynamic properties in the solid state and in solutions; to establish the curves for both solubility and the metastable limits as a function of temperature; and to determine the relationship between the solubility and the metastable limits using the acetaminophen (APAP) as a model compound. The enthalpy of fusion was determined using differential scanning calorimetry. APAP solubility at various temperatures was measured using UV spectrophotometry. The APAP solubility in water at different temperatures was measured. The activity coefficients were calculated at varying temperatures using solubility, enthalpy of fusion and melting temperature. The polythermal method was used for evaluation of the spontaneous crystallization curve of APAP. The melting temperature and enthalpy of fusion of APAP were found to be 168.3°C and 28.48 kJ/mol respectively. The standard curve of APAP was found to have a correlation coefficient value of 0.99967. Our results showed that the solubility curve, the metastable zone width, and the metastable limit curve could be predicted. The functionality of the solubility curve and the metastable limit curve were successfully determined using APAP as a model drug.

Keywords: Crystallization, pre-nucleation, metastable zone width, acetaminophen (APAP).

INTRODUCTION

Crystallization from solution is a very important phenomenon and has been used for various applications in pharmaceutical manufacturing[1-3]. The classical nucleation theory involves the existence of a critical nucleus, corresponding to the maximum of the energy vs. radius curve[4]. If such a critical nucleus does indeed exist, it would be very interesting to obtain information on its size and its structure, and compare it to the structure of the final solid formed. However, the post-nucleation events are also important and these will also influence the properties of the resulting solid[5-6]. Profound insight has been obtained over recent years by studying the crystallization of several different materials[7]. Though continuum theories of nucleation can be used to estimate the sizes for the critical nucleus and nucleation rates, they do not give detailed insight into the pathways leading from the solution to the precipitated solid[8-10]. Such information seems to be more accessible via modeling with different methods. Nevertheless, further development of continuum theories describing nucleation are still important and are being made, although these cases are typically treated on a more general level and not specifically for the crystallization from solution. This holds for classical nucleation theory as well as for continuum approaches. The simulation with different methods result in the less quantitative data involved in the process of formation of solid particles from solution compared to the continuum approaches[8,10-11]. However, nucleation from solution is rarely simulated, and it is very difficult to do: system sizes for a realistic simulation need to be quite large and molecular dynamics simulation times would need to be excessively long for a realistic description, since nucleation is a rare event[12]. Nevertheless, some reports have appeared that could give insight into the molecular level events that could lead to nucleation[13-14].

In order to gain a better understanding of how to develop particles with desired characteristics, the observation of the different stages of crystallization including the pre-nucleation stage is paramount. When a homogeneous solution reaches the state of supersaturation, clusters of molecules begin to form. Many of these clusters will be unstable and will dissolve back into solution. When a cluster, or embryo, reaches a critical size, nucleation and crystal growth will occur. The pre-nucleation stage of clustering is not well understood and may have an impact on the qualities of the resulting particles[15].

In a saturated solution, the individual molecules of a compound move between the solid phase and the solution phase; the rate of dissolution and precipitation are equal. The concentration of a solute in a saturated solution is dependent on solubility and temperature[16]. Mullin *et al*[17] demonstrated that the stable zone representing an unsaturated system is where nucleation and crystallization does not occur (Figure 1). The metastable zone between the solubility and the metastable curves represents a supersaturated solution in which nucleation and crystallization events exist; however, this is a kinetics driven process and its rate is not predictable[17-18]. The labile zone above the metastable limit represents a system which is at a level of supersaturation where spontaneous nucleation and crystallization take place.

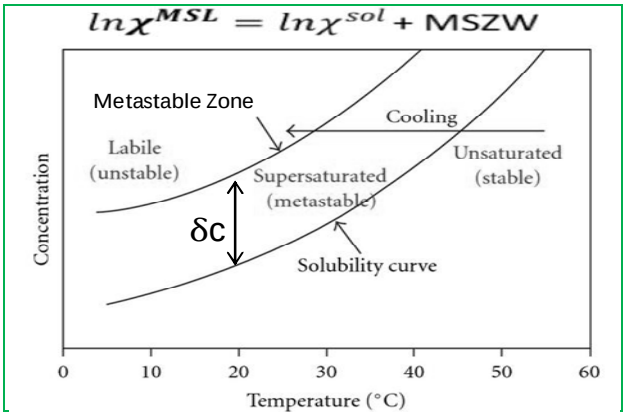

Figure 1: Solubility and metastable curve predicting the labile, stable and metastable limits and metastable zone width.

Once the concentration is high enough to reach the labile zone, nucleation and crystal growth occurs spontaneously. The purpose of the present investigation is to create a model to predict the metastable limits at a given temperature. The prediction of metastable limits allows us to further understand the pre-nucleation events without encountering spontaneous crystallization. Since the field is very wide, this study will be restricted to theoretical and modeling approaches to understand crystal nucleation and growth from solution, and to focus on the development of methods to study the stages of nucleation and crystallization reactions. We hypothesize that the metastable limit curve exhibits the same functionality as the solubility curve and that the metastable limit curve may be estimated using a data driven model. The purpose of this project is to a) determine thermodynamic properties in the solid state and in solutions; b) generate curves for both solubility and the metastable limit as a function of temperature; and c) determining what the relationship is between the two curves using APAP as a model compound. The primary goal of this study is to determine the supersaturation at a specific temperature that will allow for observation of molecular aggregation without crystallization, i.e. what level of supersaturation will fall just below the metastable limit curve. The approach presented here is to focus on pre-nucleation, the time just before crystallization begins, and to use this early stage of particle formation to predict the properties of the final solid. This approach will thus become valuable in understanding qualitative features of nucleation processes on a general as well as on a system-specific level.

MATERIALS AND METHODS

Modeling principle

In order to develop the model we have used the following concepts. If the equation of a line is $y_1 = mx + b$, and it is assumed that the functionality of a second line is the same and that it runs parallel to the first, then a model can be created based on the equation for the first line. Given that the slope would be the same at any given value for x, the only difference between the two equations would be the change in *b*, the y-intercept. So the model for the second line could be written as $y_2 = mx + (b + \delta b)$.

Based on abovementioned principle, if the equation for solubility is known then a model can be established for a parallel curve that exhibits the same functionality. We assume that the above concept will be true for metastable limits; the model would include the equation for solubility plus the change in the y-intercept. In this case the change in the y-intercept is equal to the metastable zone width. The metastable zone width is the change in concentration between the solubility and the metastable limit at any given temperature (Figure 1).

Nucleation

In an unsaturated solution, the molecules are stable and no nucleation occurs[18]. As soon as supersaturation is achieved, the frequency of molecular collisions increases and small clusters of molecules begin to form[17]. Most of the time, many of these clusters or embryos are unstable and dissolve back into solution. The formed clusters continue to dissolve into solution until an embryo reaches a critical size and becomes stable. This critical size is related to the free energy of the volume and free energy of the surface. Figure 2 shows the relationship between the volumetric energy gain, surface tension cost, and the size of the nucleus in homogeneous nucleation. Since the ratio of surface area to volume decreases with size, the growth in the size of the nucleus overcomes the surface energy cost due to the free energy gained by the added volume. Thus, the total negative free energy contributes to the nucleation process. To determine this critical point, we used the equation for free energy shown in Figure 2. G_v is the free energy change of the transformation per unit of volume and γ is the surface tension. The derivation of free energy with respect to the radius of the nucleus allows us to calculate the change in free energy at a specific nucleus size. At the critical point where the curve direction changes the derivative value becomes zero. Once the nucleation process starts and crystal growth begins it will continue until the solutions reaches equilibrium solubility.

Solubility model

In order to develop the model for metastable limits, the understanding of solubility process is very important[19]. The tendency of molecules to mix with each other is dependent on temperature, which predicts the extent of solubilization[20]. Solubility phenomena involve the forces that resist ideal mixing. Therefore, for a solid, the ideal solubility is equal to ideal mixing minus the resistance of the solid. The resistance of the solid is equal to the total energy required to break the crystal structure.

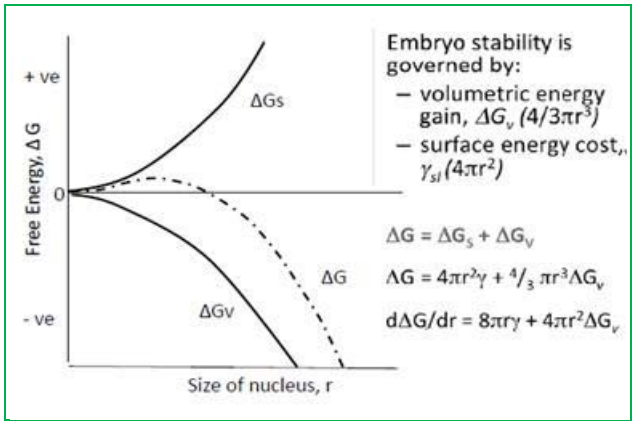

Figure 2: Relationship between the volumetric energy gain, surface tension cost, and the size of the nucleus in homogeneous nucleation.

As depicted in Figure 3, the total energy required to break the crystal lattice is equal to the energy used in heating the crystal plus the energy used in melting the crystal minus the energy released cooling the melt. Assuming the energy used in heating and the energy released in cooling are equal, the total energy required is equal to the energy required for melting the crystal, or the enthalpy of fusion (Figure 3A).

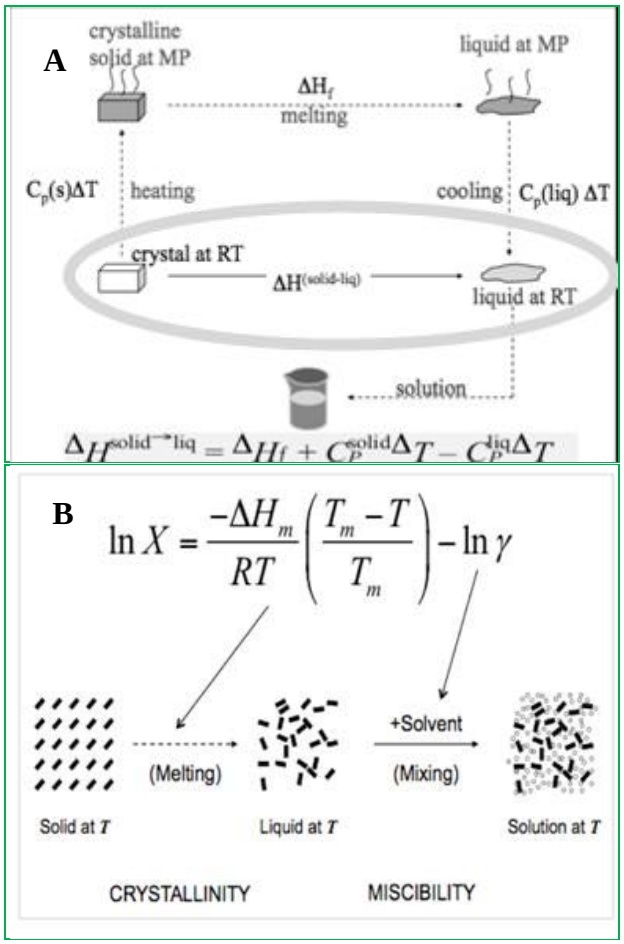

Figure 3: Solubility phenomenon involves the forces that resist ideal mixing (**A**) and crystalinity and mixing (**B,** courtesy of Rodolfo Pinal, Purdue University, West Lafayette, IN).

The resistance involved in mixing of molecules has to be considered in the calculation of real solubility[21-22]. This is the energy required to disrupt the molecules of the solvent and was accounted for in the model by the activity coefficient, γ. The model now accounts for temperature dependence, the enthalpy of fusion to break the crystal lattice, and the resistance of the liquid to mix. In order to use this model, the enthalpy of fusion and the melting temperature are calculated and the activity coefficients must remain constant with varying temperatures. Keeping the activity coefficient constant at varying temperatures allows use of the model for ideal solubility in order to extrapolate solubility at a desired temperature with a small number of experimental data points. The use of the model for ideal solubility will yield two equations for two different temperatures (figure 3B and 4). The utilization of experimental data for the solubility at T_1 and combination of two equations allows calculating the solubility at a desired T_2.

$$ln\chi_{T1} = -\frac{\Delta H_{fus}}{R}\left(\frac{1}{T_1} - \frac{1}{T_m}\right) \quad \text{and} \quad ln\chi_{T2} = -\frac{\Delta H_{fus}}{R}\left(\frac{1}{T_2} - \frac{1}{T_m}\right)$$

By combining these equations:

$$ln\chi_{T1} - ln\chi_{T2} = \left[\left(-\frac{\Delta H_{fus}}{R}\right)\left(\frac{1}{T_1} - \frac{1}{T_m}\right)\right] - \left[\left(-\frac{\Delta H_{fus}}{R}\right)\left(\frac{1}{T_2} - \frac{1}{T_m}\right)\right]$$

$$ln\chi_{T1} - ln\chi_{T2} = \left[\frac{\left(-\frac{\Delta H_{fus}}{R}\right)}{T_1} + \frac{\left(\frac{\Delta H_{fus}}{R}\right)}{T_m}\right] - \left[\frac{\left(-\frac{\Delta H_{fus}}{R}\right)}{T_2} + \frac{\left(\frac{\Delta H_{fus}}{R}\right)}{T_m}\right]$$

$$ln\chi_{T1} - ln\chi_{T2} = \frac{\left(-\frac{\Delta H_{fus}}{R}\right)}{T_1} + \frac{\left(\frac{\Delta H_{fus}}{R}\right)}{T_m} + \frac{\left(\frac{\Delta H_{fus}}{R}\right)}{T_2} - \frac{\left(\frac{\Delta H_{fus}}{R}\right)}{T_m}$$

$$ln\chi_{T1} - ln\chi_{T2} = \frac{\left(-\frac{\Delta H_{fus}}{R}\right)}{T_1} + \frac{\left(\frac{\Delta H_{fus}}{R}\right)}{T_2}$$

We get: $$ln\chi_{T1} - ln\chi_{T2} = \left(-\frac{\Delta H_{fus}}{R}\right)\left(\frac{1}{T_1} - \frac{1}{T_2}\right)$$

Figure 4: Derivation of the equation used to extrapolate solubility at desired temperature.

Differential scanning calorimetry

We used differential scanning calorimetry (DSC) to determine the enthalpy of fusion[23]. DSC measures the difference in the amount of heat required to increase the temperature of a sample compared to a reference. When the sample undergoes a phase transition it will require more or less heat flow than the reference to maintain the same temperature. This is because during phase transitions heat is either absorbed or released, depending upon the type of transition[23]. The heat flow is the difference in the amount of heat being supplied to the sample compared to the reference, i.e. the amount of heat absorbed or released during transitions. The enthalpy of fusion was calculated using the weight of the sample and the total energy absorbed using area under the curve. The melting point is the temperature at the onset of the curve.

UV-based solubility

UV spectrophotometry was used for quantitative measurement of APAP in solution[24]. Light was imaged upon a sample cuvette and a reference cuvette. The

transmitted light through the cuvette is separated into different wavelengths and focused on a detector. The peak absorbance of the sample relative to the reference was calculated. A standard curve was generated using APAP concentration in the range of 0.005 – 0.02 mg/mL. The samples of known concentration were analyzed in the spectrophotometer and absorbance values were recorded. The values were then plotted as Absorbance vs. Concentration and a linear regression line was fit to the data points.

For experimental solubility data points, excess APAP powder was added to deionized water in a 250mL, jacketed beaker with a magnetic stirrer. The temperature was kept constant using a thermostatic bath/circulator and the APAP powder in the water was allowed to equilibrate. The stirrer was turned off and time was allowed for the powder to settle. Samples were then carefully taken from the solution; dilutions were made and analyzed using UV spectrophotometry. The standard curve was used to determine the concentration of the diluted APAP samples and these values were used to calculate the concentration of the solution in the beaker at the constant temperature. These values were then plotted as Concentration vs. Temperature.

Development of a reliable sampling method was a challenge. Initially, samples were taken using a syringe and the solution was then filtered through a 0.2µm nylon membrane filter into a collection beaker. A micropipettor was used to measure the sample and transfer to a volumetric flask for further dilutions. This method seemed to be reliable until higher temperatures were reached which showed lower concentration when compared to literature values. The probable reason may be precipitation of solute during cooling in the sampling process. To overcome this problem, we have used a controlled temperature bath. An additional water-jacketed beaker was connected to the thermostatic bath/circulator. All sampling equipment was placed into the extra beaker to pre-warm before sample collection. The second method tried was to use the micropipettor to carefully take a sample directly from the solution without the use of any filters. This method was determined to be unreliable due to the inconsistency of data, as can be seen in the results section.

For the final set of data, the solution was allowed to equilibrate while stirring at constant temperature overnight. The stirrer was stopped and the mixture was kept for 4 hours to allow sufficient time for the APAP powder to settle before sample collection. The syringe, filter, and collection beaker were either warmed in an oven (30°C and higher) or cooled in a temperature bath (less than 30°C) in order to maintain the same temperature as that of the solution. In the cooling bath, the syringe and filter were kept dry in a beaker floated in the larger jacketed beaker. The samples were collected using a syringe and filtered using 0.2µM filter. The filtration was repeated to overcome the possible capacity of the filter to adsorb solute from the saturated solution, as described by Mullin et al[17]. For temperatures less than 30°C, the 3.0 cc sample was filtered and collected for further analysis. For the sample collections at 30°C and higher the syringe and filter were placed for 1 hour in an oven set to the same temperature as the solution. The micropipettor (with warmed pipette tips for samples 30°C and higher) was then used to pipette a measured quantity of solution into a volumetric flask and further dilutions were made.

Polythermal method – spontaneous crystallization curve

A known concentration of APAP and deionized water was mixed in a jacketed beaker and heated to a temperature at which the solution was unsaturated. The temperature was then decreased at a constant rate and the solution was observed for changes. The temperature at which crystallization was first recognized was recorded. This was done using varying rates of temperature decrease, stirring speeds, and concentrations. All of the data points for spontaneous crystallization in this paper were visually observed; eventually this will be done using UV sensors.

RESULTS AND DISCUSSION

DSC studies

The DSC results are displayed as a graph of Heat Flow vs Temperature (Figure 5). The onset of the curve is the melting temperature and was found to be 168.3°C (441.45 K). The area under the curve is the enthalpy of fusion and was found to be 188.38 J/g (28.48 kJ/mol). In agreement with our results other researchers also reported the similar enthalpy of fusion of APAP[12, 25]. These values are comparable with the reported values (Table 1).

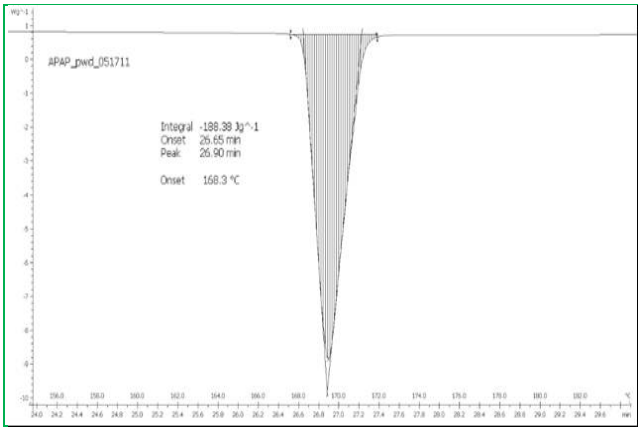

Figure 5: Differential scanning calorimetry thermogram of APAP.

Table 1: The experimental and reported values of enthalpy of fusion & melting temperature of APAP

Parameter	Literature values		Experimental values
	Picciochi et al[12]	Sacchetti et al [25]	
Tm (K)	442.1 ± 0.4	441.75 ± 0.2	441.45
ΔH_{fus} (kJ/mol)	27.2 ± 0.5	28.1 ± 2.2	28.48

Standard calibration plot of APAP

The results of the UV standard curve are shown here in the plot of Absorbance vs. Concentration (Figure 6). With a correlation coefficient of 0.99967, the standard curve was determined to be acceptable for use in the solubility measurements.

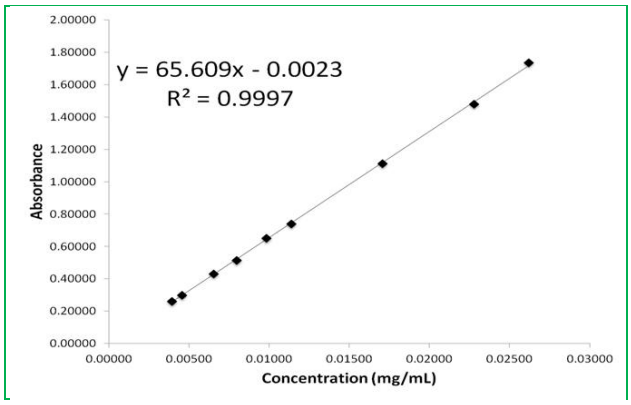

Figure 6: Standard calibration plot (Absorbance vs. Concentration) of APAP.

APAP solubility

Table 2 shows both the literature[26-27] and experimental values (mg/mL) using three methods for solubility of APAP in DI water at different temperatures. It is difficult to find literature values for solubility data for all of the temperatures in the range from 10-50°C. The experimental values were, in general, found to be lower than those reported by Mota[26], but the experimental values were similar to Granberg and Rasmuson's[27] values in the 10 to 30 °C range.

A plot of Concentration vs. Temperature including literature and experimental values is shown in Figure 7. The experimental data obtained using the second sample collection method (direct pipetting with no filter) were not comparable with the reported values and were not used for analysis.

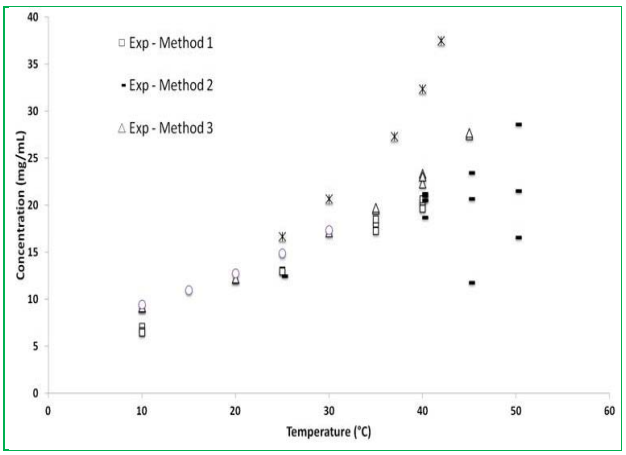

Figure 7: The comparison of literature and experimental values for APAP solubility at different temperatures.

Using the mean experimental solubility, enthalpy of fusion, and melting temperature, the activity coefficients were calculated at varying temperatures.

Table 2: The literature and experimental solubility values (mg/mL) of APAP in DI water at different temperatures

Temp (°C)	Literature values (mg/ml)		Experimental Values (mg/ml)		
	Granberg and Rasmuson et al[5]	Mota et al[4]	Method 1	Method 2	Method 3
10	9.44 ± 0.07	--	6.74 ± 0.23	--	9.14 ± 0.05
15	10.97 ± 0.09	--	--	--	--
20	12.78 ± 0.05	--	--	--	12.21 ± 0.03
25	14.90 ± 0.03	16.66 ± 1.12	13.02 ± 0.08	12.45 ± 0.04	--
30	17.39 ± 0.02	20.71 ± 0.68	--	--	17.14 ± 0.15
35	--	--	17.96 ± 0.64	--	19.67 ± 0.135
37	--	27.33± 2.97	--	--	--
40	--	32.37 ± 0.59	20.15 ± 0.46	20.4 ± 0.1	22.90 ± 0.53
42	--	37.51 ± 0.081	--	--	--
45	--	--	--	18.64 ± 6.1	27.58 ± 0.16
50	--	--	--	22.24 ± 6.05	--

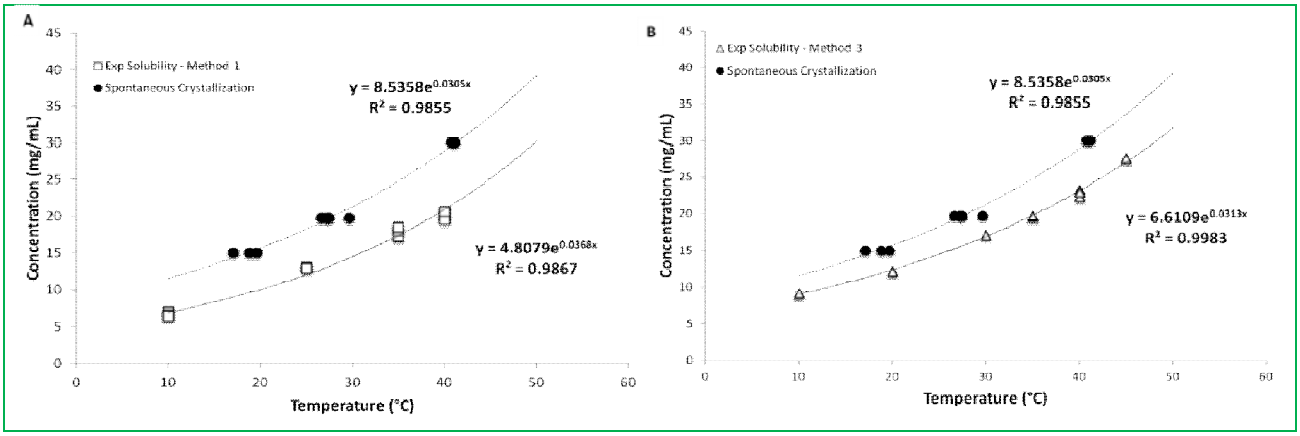

Figure 8: The comparison of solubility and metastable curves of APAP using method 1 **(A)** and method 3 **(B).**

Table 3: Activity Coefficients of APAP at different temperature

T°C	Method 1		Method 3	
	lnγ	Activity Coefficient	*lnγ*	Activity Coefficient
10	2.8	16.3	2.5	12
20			2.6	13.6
25	2.7	15.5		
35	2.8	16.3	2.7	14.9
40	2.9	17.4	2.7	15.3
45			2.7	15.1

As detailed in Table 3, the activity coefficients were constant. This supports the rationale to use the equation for ideal solubility to extrapolate data points.

The graph of Concentration vs. Temperature (Figure 8) shows the curves for solubility using method 1 (Figure 8A) and 3 (Figure 8B) and the spontaneous crystallization data are also included on each plot. An exponential curve was fit to each data set and the equations are shown. The curves can be compared using the exponential equations. Collectively these plots show the solubility limits and metastable limits for the APAP at various concentrations and temperatures. The range of values between the two curves represents the metastable zone, and distance from the solubility curve to the metastable limit curve represents the metastable zone width.

By rearrangement of the equations shown in Figure 8, the following equations are obtained:

$$\ln\chi^{sol} = 0.0368T + \ln 4.8079 \text{ ---------- (1)}$$

$$\ln\chi^{MSL} = 0.0305T + \ln 8.5358 \text{ ---------- (2)}$$

$$\ln\chi^{sol} = 0.0313T + \ln 6.6108 \text{ ---------- (3)}$$

These equations represent the mole fraction (χ) of APAP for the three different data sets: 1) experimentally determined solubility using method 1, 2) experimentally determined spontaneous solubility of Metastable Limit (MSL), and 3) experimentally determined solubility using method 3.

As the super saturation increases there will be a balance between the collision frequency and the portion of molecules whose kinetic energy is in the range to allow it to form a cluster that tips towards nucleation. For a system at higher temperature (increased solubility) the density of molecules will be greater and thus, the collision frequency increases but so does the kinetic energy of the molecules. For an increasing fraction of the distribution the kinetic energy will be "too" high for a cluster to persist, until the density increases sufficiently to out compete it. When this occurs the molecules will successfully collide, forcing the solute to precipitate out at the MSL at the higher temperature.

Our studies elaborate the methodology to evaluate the metastable limit curves, and provide advanced understanding in physical chemistry concepts that are relevant to crystallization. Furthermore, this experiment is focused on the pre-nucleation stage of crystallization, which will help to understand the molecular events during crystallization. Further work in this area could include dissolving the active pharmaceutical ingredient in an organic solvent followed by addition of water as an anti-solvent in order to reach a high enough supersaturation for nano-sized crystals to form. These nanoparticles can then be coated and used as parts of fast release dosage forms. Characteristics such as size and surface roughness of the particles formed will have an effect on the way in which they interact with each other, e.g. whether agglomeration occurs. These characteristics may be unpredictable and depend upon factors such as the degree of supersaturation as well as the specific methods used in the production process.

Our future studies will be focused on determination of spontaneous crystallization limits using UV probes. The next step in this study is to test notion that the metastable zone width is inversely proportional to solubility. A compound with higher solubility will experience a higher frequency of collisions at a given temperature in a homogeneous solution compared to a compound with lower solubility. If nucleation requires a significant number of collisions, the metastable zone width may be narrower for the compound that has a higher collision frequency. The use of data from a Concentration vs. Fraction anti-solvent curve will help to predict the formulation of nanoparticles by addition of antisolvents by assuming the metastable limit will exhibit the same parallel functionality as the solubility curve.

CONCLUSION

The functionality of the curves was found to be similar and the metastable limit curves were predictable using our proposed model. Our results predict the conditions to produce high supersaturation in order to observe molecular aggregation spectroscopically and understand the process of pre-nucleation. Additional studies need to be performed to validate the use of this model and to determine the best sampling method for the solubility studies.

Acknowledgment: The authors acknowledge the financial support provided by NSF Engineering Research Center on Structured Organic Composite Systems and College of Pharmacy, University of Hawaii at Hilo, Hilo, HI, USA.

REFERENCES

1. Erdemir D, Lee AY, Myerson AS, Nucleation of crystals from solution: classical and two-step models, , 42(5), 2009, 621-9.
2. Wang M, Rutledge GC, Myerson AS, Trout BL, Production and characterization of carbamazepine nanocrystals by electrospraying for continuous pharmaceutical manufacturing, J Pharm Sci, 101(3), 2012, 1178-88.
3. Rodríguez-Hornedo N, Murphy D, Significance of controlling crystallization mechanisms and kinetics in pharmaceutical systems, J Pharm Sci. 88(7), 1999, 651-60.

4. Yi P, Rutledge GC, Molecular origins of homogeneous crystal nucleation, Annu Rev Chem Biomol Eng, 3, 2012, 157-82.
5. Kahl G, Löwen H, Classical density functional theory: an ideal tool to study heterogeneous crystal nucleation, J Phys Condens Matter, 21(46410146), 2009, 1-7.
6. Kwon SG, Hyeon T, Formation mechanisms of uniform nanocrystals via hot-injection and heat-up methods, Small, 7 (19), 2011, 2685-702.
7. Lee AY, Erdemir D, Myerson AS, Crystal polymorphism in chemical process development, Annu Rev Chem Biomol Eng, 2, 2011, 259-80.
8. Philippe T, Blavette D, Minimum free-energy pathway of nucleation, J Chem Phys, 135, 2011, 134508.
9. Lehoucq RB, Sears MP, Statistical mechanical foundation of the peridynamic nonlocal continuum theory: energy and momentum conservation laws, Phys Rev E Stat Nonlin Soft Matter Phys, 84(3 Pt 1), 2011, 031112.
10. Di TD, De LNH, The onset of calcium carbonate nucleation: a density functional theory molecular dynamics and hybrid microsolvation/continuum study, J Phys Chem B, 112(23), 2008, 6965-75.
11. S Aubry, K Kang, S Ryu, W Cai, Energy barrier for homogeneous dislocation nucleation: Comparing atomistic and continuum models, 64 (11), 2011, 1043–1046.
12. Picciochi, R, Diogo HP, & Da Piedade MEM, Thermochemistry of APAP, Journal of Thermal Analysis and Calorimetry, 100(2), 2010, 391-401.
13. Woehl TJ, Evans JE, Arslan I, Ristenpart WD, Browning ND, Direct in Situ Determination of the Mechanisms Controlling Nanoparticle Nucleation and Growth, CS Nano, 6(10), 2012, 8599-610.
14. Anwar J, Zahn D, Uncovering molecular processes in crystal nucleation and growth by using molecular simulation, Angew Chem Int Ed Engl, 50(9), 2011, 1996-2013.
15. Farjoun Y, Neu JC, Aggregation according to classical kinetics: from nucleation to coarsening, Phys Rev E Stat Nonlin Soft Matter Phys, 83(5 Pt 1), 2011, 051607.
16. Grant DJW, Mehdizadeh M, Chow AHL, Fairbrother JE, Non-linear van't Hoff solubility-temperature plots and their pharmaceutical interpretation, International Journal of Pharmaceutics, 18(1-2), 1984, 25–38.
17. Mullin JW, Crystallization (4th Edition ed), Reed Educational and Professional Publishing Ltd. 2001.
18. Malkin AJ, McPherson A, Light-scattering investigations of nucleation processes and kinetics of crystallization in macromolecular systems, Acta Cryst, D50, 1994, 385-395.
19. Patience DB, Rawlings JB, Industrial crystallization process control, Control Systems, IEEE. 26:4, 2006, 70 – 80.
20. Fujiwara M, Chow PS, Ma DL, Braatz RD, Paracetamol Crystallization Using Laser Backscattering and ATR-FTIR Spectroscopy: Metastability Agglomeration and Control, Crystal Growth & Design, 2:5, 2002, 363–370.
21. Ikeda H, Chiba K, Kanou A, Hirayama N, Prediction of Solubility of Drugs by Conductor-Like Screening Model for Real Solvents, Chemical and Pharmaceutical Bulletin,53:2, 2005, 253-255.
22. Battino R, An Introduction to the Understanding of Solubility, J Chem Educ, 78:1, 2001, 103.
23. Clas SD, Dalton CR, Hancock BC, Differentialscanningcalorimetry: applications in drug development., Pharmaceutical Science & Technology Today, 2:8, 1999, 311–320.
24. Campanella L, Magrì AL, Tomassetti M, Rossi V, Vecchio S, Quantitative determination of acetaminophen in pharmaceutical formulations using differential scanning calorimetry. Comparison with spectrophotometric method, 33:8, 2007, 830-40.
25. Sacchetti M, Thermodynamic analysis of DSC data for APAP polymorphs, Journal of Thermal Analysis and Calorimetry, 63:2, 2001, 345-350.
26. Mota FL, Carneiro AR, Queimada AJ, Pinho SP, Macedo EA, Temperature and solvent effects in the solubility of some pharmaceutical compounds: Measurements and modeling, European Journal of Pharmaceutical Sciences, 37:3-4, 2009, 499-507.
27. Granberg RA, Rasmuson AC, olubility of APAP in pure solvents, Journal of Chemical and Engineering Data, 44:6, 1999, 1391-1395.

Source of Support: Nil, **Conflict of Interest:** None.

About Corresponding Author: Dr. Mahavir B. Chougule

Dr. Mahavir B. Chougule, is an Assistant Professor of the Department of Pharmaceutical Sciences, College of Pharmacy, University of Hawaii at Hilo. He has more than three years of Post-Doc research experiences and two years of Industrial research experience. Chougule's research focused on investigation of prenucleation and nanoparticle formulation including development of siRNA based nanoparticle systems for the treatment of cancer and pulmonary disorders. Chougule has 16 publications, 8 filed patents, 2 review article, one book chapter, and 40 scientific presentations to his credit. He is also a member of editorial board of four pharmaceutical journals. Dr. Chougule is a recipient of several national and international awards including recent American 2011 Association of Cancer Research (AACR) Minority-Serving Institution Faculty Scholar in Cancer Research Award, USA.